Jurnal Kejuruteraan 38(7) 2026: 3457-3470
https://doi.org/10.17576/jkukm-2026-38(7)-24

Experimental Optimization and Predictive Modeling of Ultrasonic Remediation of Used Cooking Oil–Contaminated Sand

Nur Ain Samat[a], Nur Shahirah Nasir[a], A.S. Alikasturi[a], Nuha Awang[b], Azzyati Johari[b], S.O. Alaswad[c], Eko Supriadi[d], Z.A. Zulhafiz[e] & M.R. Aliff Radzuan[a*]

[a]*UniKL MICET, Lot 1988, Kawasan Perindustrian Taboh Naning, 78000 Alor Gajah, Melaka Malaysia*

[b]*UniKL MITEC, Persiaran Sinaran Ilmu, Bandar Seri Alam, 81750, Masai Johor Malaysia*

[c]*Nuclear Technologies Institute (NTI), King Abdulaziz City for Science and Technology (KACST), Riyadh, Saudi Arabia*

[d]*Department of Renewable Energy Bioprocess Engineering Technology, Politeknik ATI Padang, Padang, West, Indonesia*

[e]*School of Computing,Engineering & Digital Technologies, Teesside University, Middlesbrough, UK*

[*]*Corresponding author: aliffradzuan@unikl.edu.my*

Received 24 December 2025, Received in revised form 20 June 2026
Accepted 20 July 2026, Available online 30 October 2026

ABSTRACT

Used cooking oil (UCO) released into the environment can contaminate sand and create persistent remediation challenges. This study evaluates ultrasonic treatment as a practical approach for removing UCO from oil-contaminated sand and develops a predictive model for estimating removal efficiency. A central composite experimental design comprising 52 runs was employed to investigate the effects of treatment time, ultrasonic power, aqueous medium, and oil–sand ratio. Residual oil concentrations before and after treatment were quantified using ultraviolet–visible (UV–Vis) spectroscopy, while thermogravimetric analysis (TGA) was used to support the observed removal trends. The results demonstrated that removal efficiency was strongly influenced by the combined operating conditions. The highest removal efficiency of 41.4% was achieved at 240 W, 15 min, an oil–sand ratio of 1:0.5, and saline water, whereas the lowest efficiency of 1.3% occurred at 120 W, 5 min, a ratio of 1:1.5, and tap water. Increased treatment time, ultrasonic power, and salinity generally enhanced oil removal, while the oil–sand ratio showed the strongest influence in the regression analysis. A linear regression model was subsequently developed to predict removal efficiency within the investigated operating range, achieving a root mean square error (RMSE) of 2.73. These findings demonstrate the potential of ultrasonic treatment as a controllable remediation technique for UCO-contaminated sand and provide a quantitative basis for further process optimization and scale-up.

Keywords: ultrasonic remediation, used cooking oil, oil contaminated-sand, process optimization, predictive modeling,

INTRODUCTION

There are significant detrimental effects on the chemical and physical properties of the surrounding sand caused by oil spills in rivers, seas, or streams. This may happen during oil leakage during oil exploration, production, or transportation a major problem on a global scale (Abousnina and Lim Allister 2022). There were three harmful risks posed by the incident: those to human health, the environment, and the economy (Peng et al. 2020). An ecological threat is when a variety of marine creatures, such as microalgae and invertebrates, experience growth inhibition and abrupt mortality because of the contamination (Zhou et al. 2019). Polycyclic aromatic hydrocarbons (PAHs) and heavy metals are persistent in the environment and are usually the main pollutants that accompany spills or leaks (Fraiese et al. 2020a).

Hydrocarbon petroleum and cooking oil are the most widely available oils, both of which are readily available in multiple forms and substantial quantities at once.

Petroleum hydrocarbons can infiltrate the soil via leaks and spills from refineries, manufacturing facilities, power plants, distribution depots, retail service stations, and transportation (Befkadu and Chen 2018; Zhao et al. 2021).

The next easily accessible oil as mentioned above was cooking oil. According to statistics from the EPA Biodiesel (2011), used cooking oil from restaurants was collected at almost three billion gallons annually. The United States is recognized as the largest producer of used cooking oil with 10 million tons annually, or 55% of global output. Ireland has the lowest-ever output of used cooking oil, producing only 1%, or approximately 153,000 tons per year. According to Nur Aifa Wan Azahar et al. (2016) Malaysia produces 3% of the world's used cooking oil each year. The reports by Daud et al. (2020) and Kamaruzaman et al. (2022) explained that Malaysia has an estimated 50,000 tons of cooking oil away from adequate treatment per year that are thrown into the environment. Used cooking oil (UCO) has been contaminated with several different compounds and may be dangerous for the environment. Among the various component of UCO is glycerol ester (GE). This GE contains many important fatty acids that can only be dissolved using organic solvents. Because of their potential toxicity, many countries have enacted a few environmental legislations to ensure the proper disposal of oils (Daud et al. 2020). It is difficult to remove the UCO from the contaminated sand without an appropriate procedure (Aliff Radzuan et al. 2022).

Recently, many researchers have focused on hydrocarbon petroleum as the main pollutant in their studies (Fraiese et al. 2020b; Li et al. 2020; Mat-Shayuti et al. 2021; Sivagami et al. 2019), whereas this study will use ultrasonic equipment to remove used cooking oil that sticks on the sand. Only a few scientific studies have tested other than petroleum hydrocarbon in their ultrasonic studies (Choi, Lee, and Son 2021; Dehghani et al. 2023; King et al. 2019; Mohamed Noor et al. 2022). In comparison to other remediation procedures that are currently available on the market, the ultrasonic method is the most cost-effective. Ultrasonic equipment is thought to be environmentally friendly, affordable, and easy to use. Ultrasonic machines produce sound at high frequencies typically above 20 kHz that are inaudible to human ears. The method uses ultrasonic waves to create high temperature and pressure cycles, which can separate contaminants from the soil particles (Ossai et al. 2020). To compare, Befkadu and Chen (2018) used ultrasonic irradiation to treat effluent in the soil-washing process. It uses ultrasonic pulses to create cavitation bubbles in the medium. The bubbles are then compressed, resulting in localized high temperatures and pressures. This phenomenon helps break down pollutants from the soil (Checa-Fernández et al. 2022). Effendi et al. (2019) stated in their study that ultrasonic energy causes local turbulence, which may aid in the breakdown of the soil matrix and the expulsion of pollutants from soil particles.

Ultrasonic is a known method used to enhance the mass transfer of the process (Fagan and Weavers, 2019) as well as to enhance the oil recovery (Avvaru et al. 2018). Therefore, the objectives of this study were to investigate the four main factors thought to influence the efficiency of the ultrasonic remediation process and to develop an optimization equation that can forecast removal efficiencies. This algorithm will consider the characteristics analysed, such as salinity, oil-sand ratio, retention time, and ultrasonic power to predict the best conditions for efficient remediation.

METHODOLOGY

This investigation was divided into two stages: experimental work and statistical modeling to anticipate removal efficiencies. To prepare the sample, roughly 5 kg of beach sand from Pantai Pengkalan Balak, Melaka, and 10 litres of UCO from household consumption were collected. These amounts were sufficient to be used for the entire study. The sand and UCO samples obtained are stored in a dedicated area since numerous variables can influence the quality of the oil and sand over time. The UCO may influence the quality of the remediation because oil is exposed to the environment, it may be oxidised at a high rate, making the UCO more viscous and harder to remove using ultrasonic. However, a thorough pre-treatment of the oil was not conducted as the purpose of the paper was to mimic out how untreated used cooking oil affected the remediation in real life case scenario as much as possible. So, if there were any pre-treatment done, there will be several tests to be done to confirm out properties of the oil before and after it has been pre-treated on either removal of water or other impurities. Either way, pre-treatment and careful storage consideration of raw materials are needed in another situation that might be possible. For this research paper, the storage of the raw materials is as per mentioned above was at a dedicated area which was at a non-direct light area and non humid area, to reduce the other side effect of raw materials.

The Design Experiment offers two designs: the Central Composite Design (CCD) and the Box Behnken (BB). Central Composites designs can accommodate a complete quadratic model. They are commonly employed in the planning of sequential experimentation because they can combine data from previously conducted factorial experiments. Box-Behnken designs often have fewer trial locations than Central Composite designs. Box-Behnken

designs can accommodate three levels, while Central Composite designs can handle up to five levels per factor. Furthermore, Box-Behnken designs do not contain experimental runs in which all components are set to their maximum values. However, for this experiment to obtain all the runs that are available for all parameters as mentioned in Table 1, the CCD was used.

The central composite design is believed to be the most popular response surface design experiment. A set of axial points, also known as star points, is added to a factorial or fractional factorial design with central points to calculate curvature. Central composite designs, which include the centre and axial points of previously completed factorial designs, are utilized to successfully estimate first- and second-order terms and represent a curvature response variable. Their specific application is demonstrated in the context of sequential experiments, in which earlier factorial experiments can be enlarged by introducing axial and centre points. Box-Behnken designs, on the other hand, do not include axial points, hence all design points fall within the stipulated safe operating ranges.

TABLE 1. Full factorial run for sand samples in the ultrasonic machine

Parameters	Units	Variable	Factors
Oil-Sand Ratio	g/g	1:0.5, 1:1.0, 1:1.5	Numeric
Experimental Time	minutes	5, 10, 15	Numeric
Ultrasonic Power	watt	120, 240	Categoric
Salinity	g/g	Tap water, Saline water	Categoric

The materials were analysed using Fourier Transform Infrared (FTIR) Spectroscopy, Ultraviolet Visible Spectroscopy (UV-Vis) and then validated using Thermogravimetric Analysis (TGA). The results were then utilized to generate the optimal equation for predicting the most accurate RE of oil from oil-contaminated sand. The concentration of oil in the sand before and after treatment was determined using UV-Vis analysis. Finally, the TGA analysis was utilized to measure the weight loss of the sand before and after treatment, as well as to estimate the RE.

RESULTS AND DISCUSSION

Thermo Fisher Scientific FTIR Nicolet iS10 was employed as a critical pre-analysis step to identify the functional groups present in the contaminated sand samples. The chemical characterization of the oil and the sand was only done through the usage of Fourier Transform Infrared (FTIR) as they somehow affected the remediation efficiency at certain level of parameters which can be seen throughout the paper.

Firstly, the drying oven will be turned on and set at 150°C and let to heat up. On the other hand, the sample sand will be fully blended for at least 5 minutes before being weighed and left away. Next, 0.1g of spent cooking oil will be weighed and mixed with the fine sand. The oil-sand combination will next be pestled in a mortar with 0.1g Potassium Bromide (KBr) powder until fully ground. Next, the sample will be placed in the pre-set drying oven for over an hour to dry, and 1g of the entire mixture will be scooped into the sample pellet ring. Only then will it be hydraulically forced down, and the sample pellet ring will be put into the FTIR chamber to perform the analysis.

The FTIR spectra revealed distinct peaks corresponding to alkenes, esters, alkanes, and silicates, confirming the presence of used cooking oil on the sand. The peaks at 3131.43 cm^{-1} (alkene C-H stretching), 1743.08 cm^{-1} (ester C=O stretching), 1625.26 cm^{-1} (alkene C=C stretching), and 1400.83 cm^{-1} (alkane C-H bending) indicated the presence of oil. Additionally, peaks at 1085.03 cm^{-1} (Si-O stretching), 786.34 cm^{-1} (Si-O-Si bending), and 462.94 cm^{-1} (Si-O bending) confirmed the presence of silicates, indicative of sand. This analysis was crucial to ensure that the samples were predominantly contaminated with oil, avoiding interference from other potential contaminants. By identifying these characteristic functional groups, the study validated the chemical nature of the contamination, setting a solid foundation for subsequent remediation experiments (Sivakumar et al. 2012).

Table 2 and Figure 1, exhibit the details of the FTIR analysis for the UCO and sand samples.

TABLE 2. Details of peaks from the graph

Wavenumbers (cm^{-1})	Types of vibration	Nature of Functional Group
3131.43	=C-H stretching	Alkene
1743.08	C=O stretching	Ester
1625.26	C=C stretching	Alkene
1400.83	C-H bending	Alkane
1085.03	Si-O stretching	Silicates (Silicon Dioxide – sand)
786.24	Si-O-Si bending	Silicates
462.94	Si-O bending	Silicates

UV-VIS ANALYSIS CALIBRATION CURVE

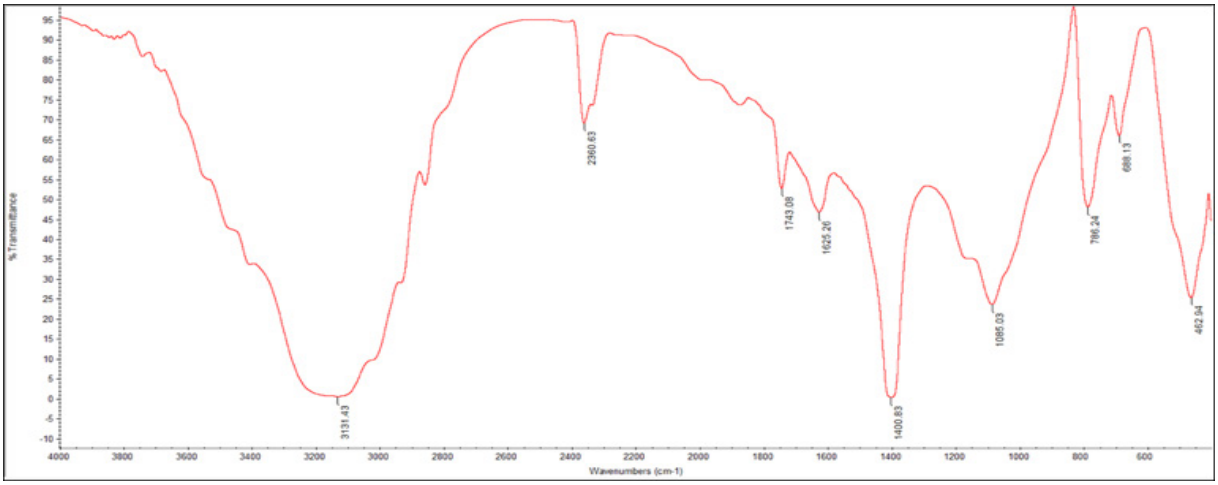


FIGURE 1. FTIR of UCO and Sand sample

The PerkinElmer UV-Vis model Lambda 750 was used to analyse the pre-and post-treatment sand samples by measuring absorbance intensity. First, a calibration curve was constructed to assist in the precise estimation of the oil concentration in the samples. The calibration curve illustrates a method for correctly predicting an analyte concentration in unidentified samples by correlating observed responses to known standard values. This is to determine unknown sample concentrations. Interpolation or extrapolation of concentration can be achieved by measuring the unknown sample's response and comparing it to the calibration curve. The calibration curve was constructed using all the raw data from the absorbance and calculated using Eq. 1.

$$C_{oil} = \frac{a + 0.0761}{0.0802} \quad (1)$$

The best absorbance response was obtained at 269 nm wavelength. The calibration curve for the used cooking oil yielded linear lines of best fit, as mathematically defined in Eq. 1 with the R^2 value of 0.997. Here *a* is the absorbance value obtained from the UV-vis. Figure 2 depicts the calibration curve generated from the serial dilution data done on the UCO sample.

The main protocols for using the UV-Vis spectrophotometer with the solvent extraction method were described by Agarwal et al. (2016); Aliff Radzuan et al. (2016). Sand samples weighing 1g each were collected from the ultrasonic bath and were submerged in 10 mL of hexane in a 100ml beaker. After shaking the samples gently for 5 minutes and allowing them to settle, a layer of hexane and dissolved oil formed on the surface. A pipette was then used to transfer 10 ml of the hexane-oil mixture from the beaker to the UV-Vis cuvette. This cuvette was placed in the UV-Vis spectrometer, alongside another cuvette that contained only pure hexane. The extracts were then transferred to cuvettes for UV-Vis analysis at 269 nm wavelength.

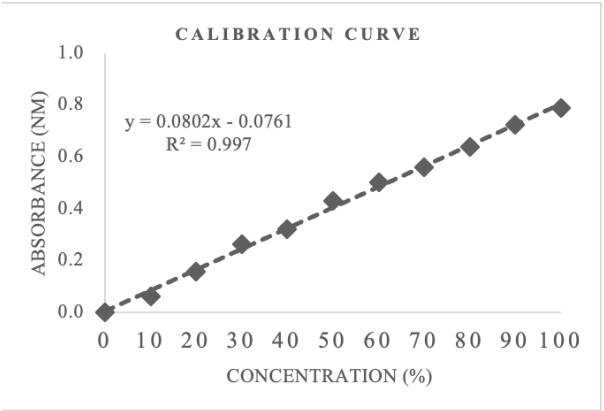


FIGURE 2. Calibration Curve of UCO

FACTORS AFFECTING REMOVAL EFFICIENCY (RE)

RETENTION TIME

The retention period was the first component controlled in this research investigation. In other words, retention time refers to the amount of time a specific material or reactant spends going through the sonication process in an ultrasonic reactor. In theory, the RE should increase over time. Based on Figure 3 and Figure 4, Blackstone, (2013) theory in his early research lends validity to this conclusion. There were various reasons why the increase of time equalled an increment of RE, such as when a high-

amplitude ultrasonic transducer vibrates, the liquid medium absorbs the energy and begins to oscillate, creating a shearing force. As a result, mass transfer increases and the sand's surface is cleaned.

These figures also show the relationship between RE and Time will be assisted by the medium solution and ultrasonic power. The increment of RE against the increment of time can be noticed on all runs. This was because an extended period of oil-sand in the ultrasonic reactor permitted extended surface contact with micro jetting of microbubbles to the oil surface which breaks down more oil particles against the sand surface. Although, Feng & Aldrich, (2000) mentioned that after five minutes of sonication, there will be a significant decrement in diesel oil removal because of the oil's re-adsorption. Therefore, to prevent re-adsorption of the oil, the oil-water emulsions should be removed from the sand while the desorption is at its maximum. However, according to these figures, there was no decrease in efficiency even five minutes into the experiment. This could be related to the use of ultrasonic, which was more delicate and higher in frequencies than sonication.

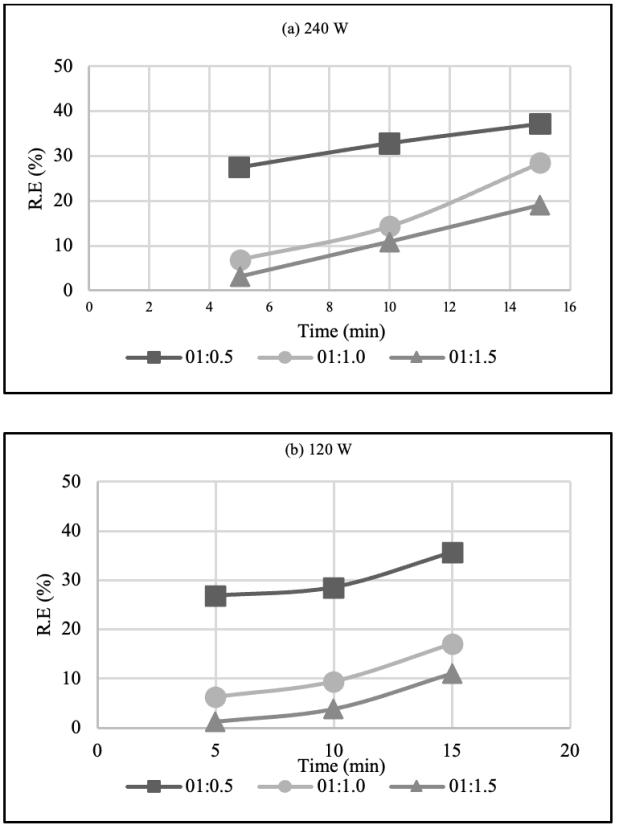


FIGURE 3. RE vs. Time for Tap water at Power (a) 240 W & (b) 120 W

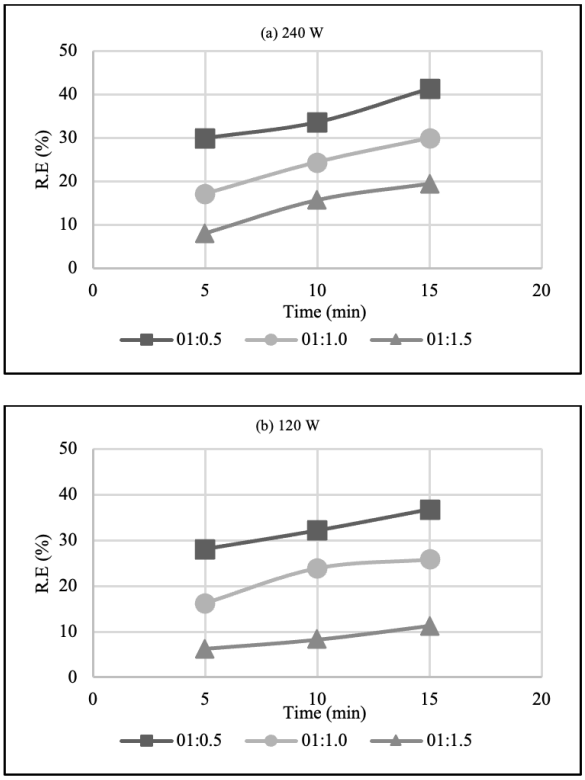


FIGURE 4. RE vs. Time for Saline Water at Power (a) 240 W & (b) 120 W

Another reason a longer retention time contributes to greater removal is that some oil may become trapped inside the sand matrix, depending on the oil's viscosity and the size of the sand grains. Extended ultrasonic treatment boosts sound wave penetration and cavitation energy penetration further into the sand, potentially helping to release trapped oil (Xu et al. 2017). In cleaning applications, minimal agitation offers various benefits, including fast interruptions that assist weaken the internal links of oil molecules by disrupting the cohesive forces between them. Furthermore, the motion decreased the forces of adhesion between the oil and sand particles. This combined action facilitates the separation of oil contaminants from the sand and promotes effective cleaning (Yusof et al. 2016). Although this was only a discussion about RE vs. Time, there should be a disclaimer about the limitations of time in the ultrasonic remediation method and to not only focus on this one factor but also focus on other factors because, as mentioned by Park and Son, (2017) time assisted by other factors, considering variables like power generation, length of treatment, and sand characteristics, we can remove the required amount of oil in an appropriate amount of time. Jatnika Effendi and Wulandari (2019) explore the effect of time in their paper, using TPH, oil, and grease as samples. According to the data acquired, the TPH value decreased by 45.48% at minute 13. Additionally, it was

stated that 10 to 15 minutes was the optimal amount of time for ultrasonic treatment. Fraiese et al. (2020), who investigated electrokinetic and ultrasonic remediation setups, found that an average clearance of 88% was found after just 5 minutes of sonication; however, practically total elimination was seen when the treatment period was extended to 10 minutes.

SAND-OIL RATIO

This experiment used three different ratios that comprises w/w% of oil and sand where there were 1 to 0.5 ratio, 1 to 1.0 ratio, and 1 to 1.5 ratio as demonstrated in Figure 5 and Figure 6. This ratio factors were chosen because they do have an impact on the remediation using ultrasonic on oil in sand (Wulandari & Effendi, 2018). The underlying process in ultrasonic was cavitation, in which tiny bubbles in the oil-water mixture were produced and burst by ultrasonic vibrations, resulting in microjetting. The enormous shear pressures of collapsing bubbles cause oil droplets to split apart, increasing their surface area and enhancing contact with sand particles. As a result of the reduced oil-to-sand ratio, there was more sand surface area available for oil droplet contact (e.g., 1:0.5). This makes it possible for the sand particles to successfully catch more oil during cavitation. On the other hand, a larger oil-to-sand ratio (such as 1:1.0 or 1:1.5) might prevent effective collection since there would not be enough sand surface area for all the oil droplets (Dabirian et al. 2018).

Higher viscosity oil was thicker and less prone to breaking apart when cavitation bubbles collapse. This may reduce the effectiveness of oil removal, especially when dealing with bigger oil droplets. Although there was no difference between the chemical composition of the unused and used cooking oil as mentioned in the FTIR section, the viscosity of the used cooking can be seen to be more viscose than the unused cooking oil due to several ingredients such as fish fat and other fats got mixed during cooking.

At larger oil-to-sand ratios (such as 1:1.0 or 1:1.5), the detrimental effects of high viscosity are probably going to be more apparent. The heavier oil droplets may find it more difficult to disperse when there is less sand surface area available, which would further impede clearance. High-viscosity oil has trouble flowing and dispersing effectively in combination containing sand. Larger oil droplets that are unable to effectively come into touch with enough sand surface area may result from this, clumping or otherwise. As a result, as the sand slurry viscosity increased with the soil ratio, so did sound energy consumption and attenuation, generating difficulties in cavitation and the weaker cavitation bubbles pressure, which was unfavourable for pollutant desorption from oil.

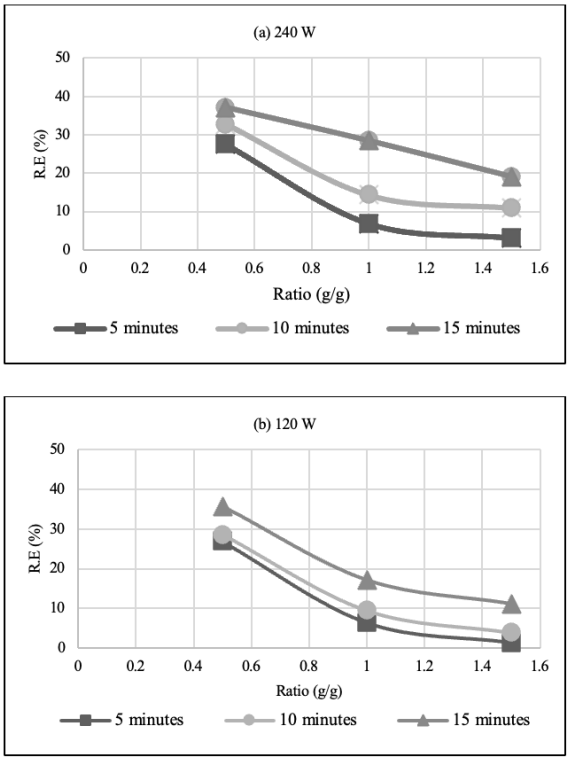


FIGURE 5. RE vs. Ratio for Tap water at Power (a) 240 W & (b) 120 W

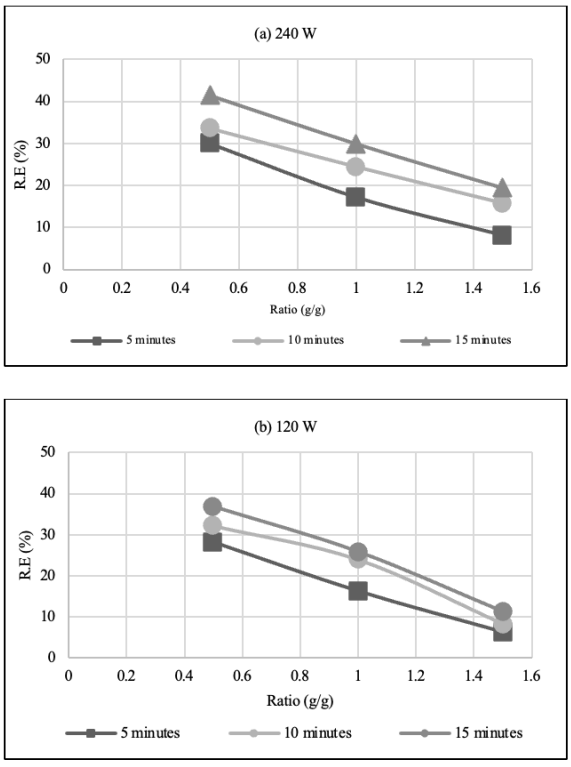


FIGURE 6. RE vs. Ratio for Saline Water at Power (a) 240 W & (b) 120 W

ULTRASONIC POWER

The next significant factor was ultrasonic power. The total amount of power used in this research experiment was 120 W and 240 W which inevitably converts to full ultrasonic power and half ultrasonic power. Ultrasonic power is electrical energy that is converted into high-frequency sound waves for use in a variety of applications using a piezoelectric transducer and ultrasonic generator.

Increased power often corresponds to increased vibrational amplitude which causes the cavitation bubble to collapse more forcefully, raising the temperature and pressure. An increase in ultrasonic power causes cavitation, which causes an increasing number of bubbles to develop and burst in the oil-sand combination. In the experiment, there were two levels of power used which were 120 and 240 watts. Figure 7, Figure 8, and Figure 9 demonstrate that as the power increases the RE also increases. Although there are some limitations where when power exceeds the limit, it was not applicable in this research study as there was no sudden drop of RE in the graph. This was because the range of the power used in this experiment was still within the optimum factor where the sudden drop was not observed.

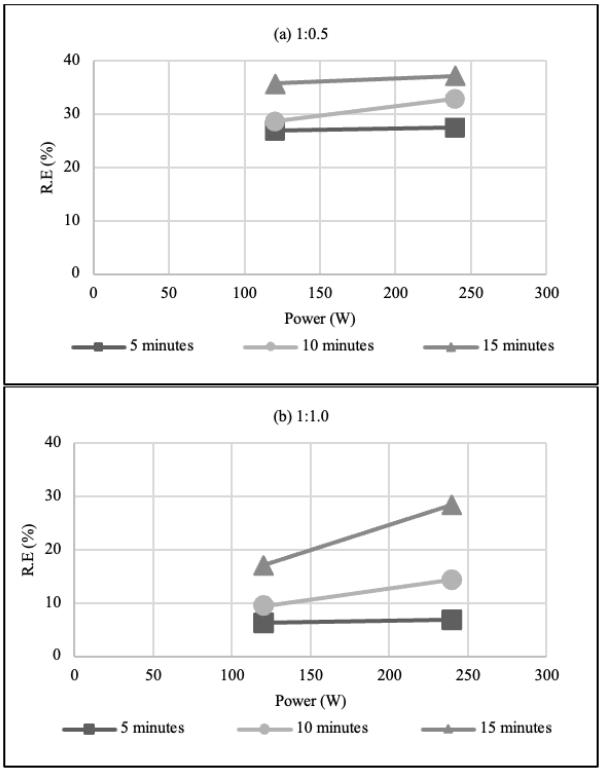


FIGURE 7. RE vs. Time for Tap water at Ratio (a) 1:0.5 & (b) 1:1.0

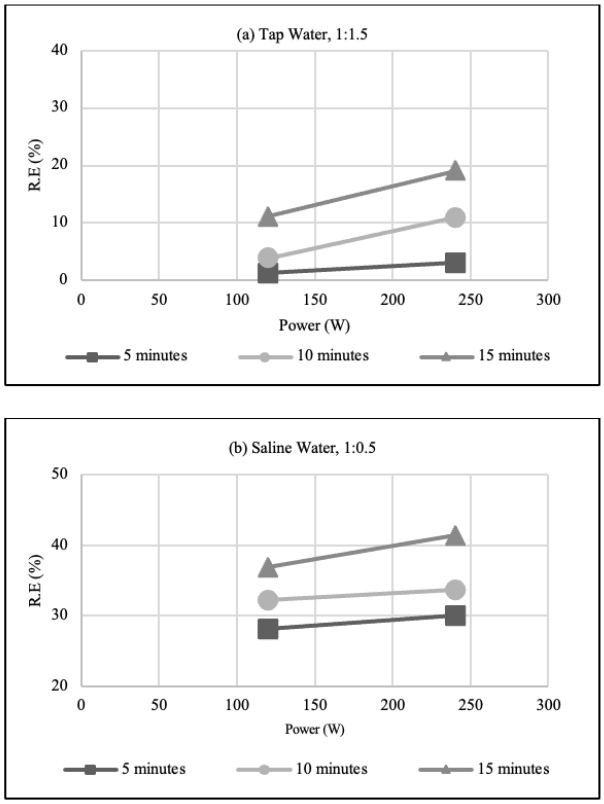


FIGURE 8. RE vs. Time Tap & Saline Water at Ratio (a) 1:1.5 & (b) 1:0.5

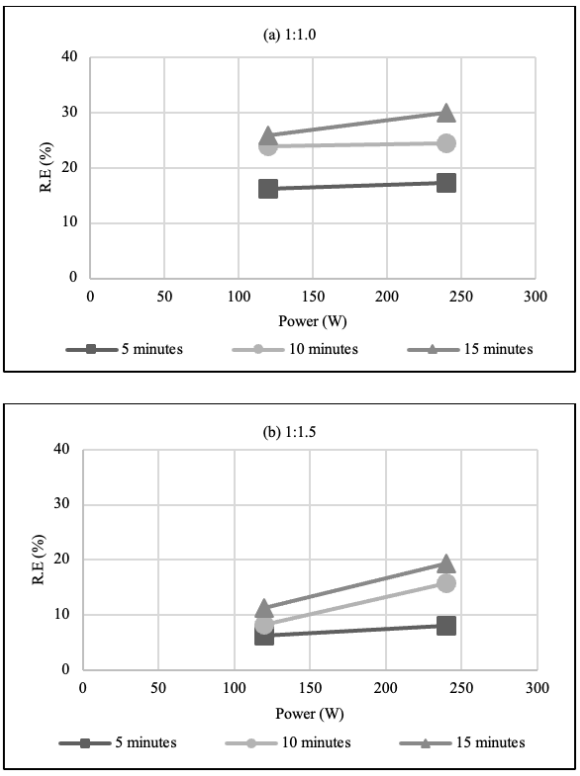


FIGURE 9. RE vs. Time Saline Water at Ratio (a) 1:1.0 & (b) 1:1.5

Better oil recovery was usually achieved due to the the strong micro-jets and shockwaves produced by this severe cavitation. Hence, successfully separated oil droplets from the sand particles. The cavitation-induced agitation enhances the solvent molecules' mobility in the oil-sand combination which will help in improved mixing and makes it possible for the solvent to reach more oil and encourages its separation from the sand. To summarise, higher power amplitude will increase the number of cavitation bubbles, the temperature of collapse, and the sonochemical yield and will be directly correlated with the power delivered to the liquid (Effendi et al. 2019).

Higher powers have been shown to enhance the number of active cavitation bubbles in sonochemical processes, indicating that pressure amplitude plays a significant role. There is a limit for excessive powers where there is a decrease in the number of active bubbles per unit volume, even though sonochemical yield increases at greater powers. More power increases have the potential to cause excessive bubble development at a certain point where these bubbles have the potential to grow so tiny and numerous that they begin to interact with one another, impeding their final collapse. The phenomenon can be referred to as bubble coalescence suppression (Drozdov et al. 2017). This was where the capacity of bubbles to separate oil from sand particles was greatly reduced when they were unable to expand and contract with efficiency. Because of this, even if the power is still strong, the efficacy of oil removal drops suddenly.

Mat-Shayuti et al. (2021) in their paper mentioned that in an experiment where the contaminated oil either in a suspended configuration or placed at the bottom was remediated for 10 minutes of running, at 30 to 120 Watt (W) of power, 25 to 60 kHz of frequency, and 10-100 g of sand load, the highest frequency of 60 kHz was the ideal setting for suspended samples and the ideal frequency was at 28 kHz. Also, an abrupt increase in power might mess with bubble dynamics because it causes bubbles to expand erratically, leading to poor cavitation and material (bubble) growth. Therefore, it can be noted that the frequency should not be varied while undergoing an experiment and instead focus on which has been mentioned to be the most effective.

Although both power values were used for this research which was at 120W and 240W, the frequency selection available from the ultrasonic equipment were only at around 40 Hz based on manual provided. Both power and frequency here does correlate whereas the power increases, the frequency increases with the limitation coming from the equipment itself as it provides the end user with only these two selections. Although that, there were no calibration and verification from the user side regarding the exact power and frequency supplied throughout the experiment as the manual for the machine was provided. Therefore, to increase the accuracy for the overall experiment for future researcher, this can be look into and further studied to reduce the limitation in this literary sense.

MEDIUM

The next factor that can be discussed is the medium factor. In this experiment, there were only two levels of salinity used which were tap water and saline water. The Syarikat Air Melaka Berhad (SAMB) supplied the tap water, and the saline water was prepared specially for the experiment where 3.5% of salt was used in a litre of solution which was tap water. The 3.5% used was due to the fact to mimic the ocean salinity level. Aliff Radzuan, (2017) in his dissertation mentioned that the removal of hydrocarbon oil increased when salt was present. Although that, some issues needed to be addressed. Due to the minimal amount of literature review that talks about the effect of salinity on a solution that will be undergoing ultrasonic remediation, the possible reason why the higher the salinity, the better remediation was because of surface tension. The characteristic of a liquid surface that resembles a stretched elastic membrane is called surface tension. The cohesive forces between molecules at the liquid's surface are the cause of this phenomenon. When salt and water react, salt will separate into ions such as sodium and chloride ions from NaCl. In general, saline water offers certain benefits over tap water when it comes to cleaning up oil-contaminated sand. When salts are dissolved in saline water, the water becomes denser and more viscous. This increases cavitation during ultrasonic cleaning, causing microbubbles to develop and burst more forcefully. The removal of oil pollutants from the sand surface might be more successful because of this increased cavitation activity.

Another reason saline water was better than tap water was due to the Reynolds number. In fluid dynamics, the Reynolds number (Rey) was used to describe the flow regime surrounding a particle such as a microbubble. It assists in identifying whether inertial forces are dominating the flow around the bubble. Eq. 2 shows the formula for Rey and some of the factors affecting Reynold's number. Based on the Reynolds number theory, the larger the bubble the higher the Re value. The next factor was bubble rise velocity where the faster the bubble rise, the higher the Re value. Another one was viscosity where the more viscous the solution, the lower the Rey value. The last factor was the density, which the denser the liquid, the lower the Rey value.

$$\text{Rey} = \frac{\rho L \times Vz \times d}{\mu L} \quad (2)$$

Here, ρL is the density of the liquid, Vz is the bubble velocity, d is the diameter of the bubbles, and μL is the viscosity of the liquid. Based on Figure 10, Figure 11, and Figure 12 shown, the RE value against salinity does increase whether it was with the ratios of 1:0.5, 1:1.0, or 1:1.5 and whether it was at 240 W or 120 W.

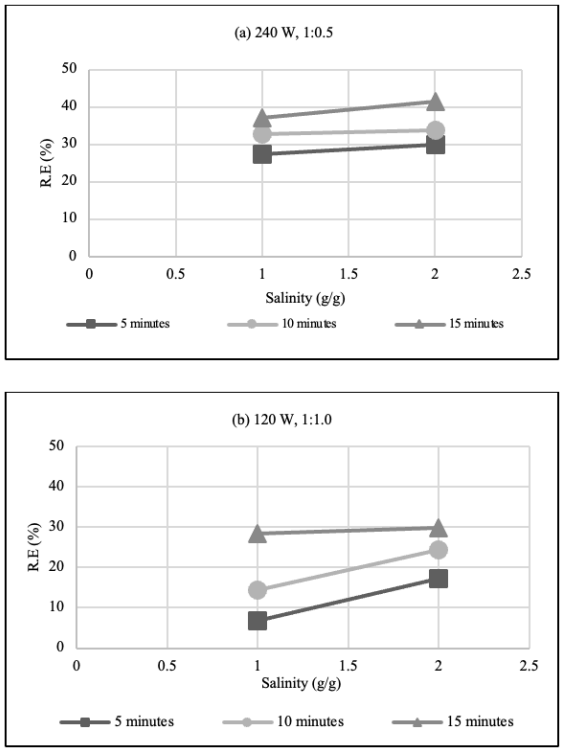


FIGURE 10. RE vs. Time for Tap water at Ratio (a) 1:0.5 & (b) 1:1.0

Although the observation of Rey was not done in this study, the theory itself can help us better understand why the saline water was better in terms of ultrasonic remediation of oil and sand rather than using tap water only. When cavitation occurs in the ultrasonic, microbubbles are created which will rise inside the medium. As saline water was more viscous than tap water, the bubble mean size formed due to the cavitation, being smaller (C.W. Engelsen et al. 2002; Jamil et al. 2021) and reducing the chances for the bubble to coalescence and agglomerate together (Aliff Radzuan et al. 2016). Therefore, when bubble size decreases and the chances of coalescing bubble decrease, the terminal rise velocity of the bubble decreases as it does not change in terms of size.

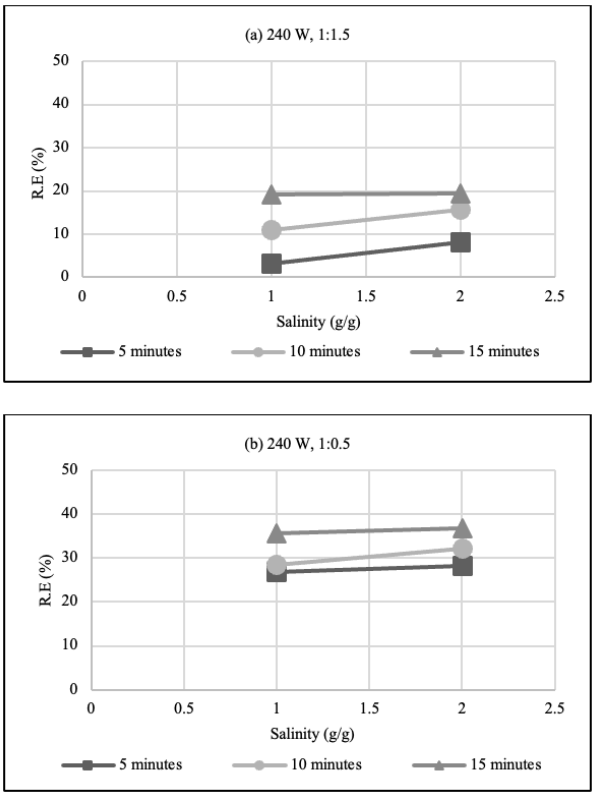


FIGURE 11. RE vs. Time Saline Water at Ratio 1:1.5 & 1:0.5

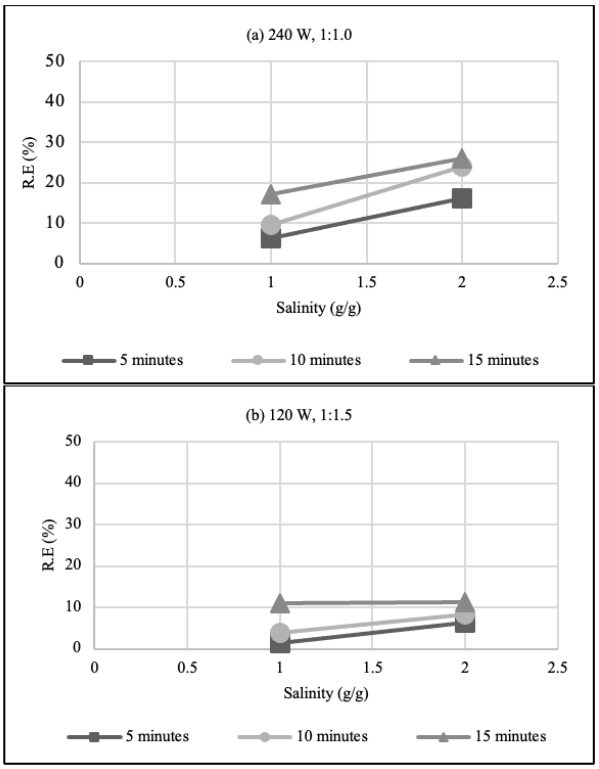


FIGURE 12. RE vs. Time Saline Water at Ratio (a) 1:1.0 & (b) 1:1.5

This was supported by Kováts et al. (2020) who in his paper, mentioned that the terminal bubble velocities in solutions decrease in velocity as viscosity increases. The higher the terminal rise velocity, the shorter the retention time inside the ultrasonic. This was because the dragging force of smaller bubbles was lesser than larger bubbles as mentioned by Rashid et al. 2023. More cavitation cycles have more chances to extract UCO from the sand and were made possible by a longer retention period as it gave more time for the bubbles to be attached to the oil and rise to the surface of the medium. This implies that improved cleaning efficiency does benefit from a longer retention period. All over, salinity does play a huge impact in the effect of remediation using an ultrasonic approach.

REGRESSION AND CONTOUR PLOT

The linear regression model includes all of the experimental data. Data was correlated using linear regression, as offered by the Microsoft Excel® Analysis Toolpak option. All the graphs presented showed little curvature and were the simplest way to match the data, requiring the fewest parameters to be computed and so adhering to Ockham's razor. The linear regression is defined in mathematical form as in Eq. 3.

$$\mathrm{RE}(\%) = \mathrm{Y} + \mathrm{T}\alpha + \omega\beta + \Omega\gamma - \Theta\delta \quad (3)$$

Here, Y is the intercept value at the Y-axis, α represents time (minutes), β represents power (watts), γ represents salinity, and δ represents the sand-oil ratio. The value of each coefficient calculated from the linear regression was found to be Y=-26.206,T=1.067,ω=0.0265,Ω=7.680 ,Θ=16.144.

The positive equation indicates that the dimensionless group is directly proportional to the removal efficiency, whereas the negative equation implies the opposite. This linear regression demonstrates that the sand-oil ratio has the largest influence on removal efficiency as it has the largest values.

The parity plot (see Figure 14) was used to investigate the quality of fit of the linear regression. The root mean square effort of this linear regression was determined to be 2.73 using Eq. 4. Here, RE_a, RE_p and N are actual removal efficiency, predicted removal efficiency and number of samples, respectively. The correlation is strictly limited to settings identical to those employed in our experiments.

$$RMSE = \sqrt{\sum_{i=1}^{N} \frac{(RE_a - RE_p}{N}} \quad (4)$$

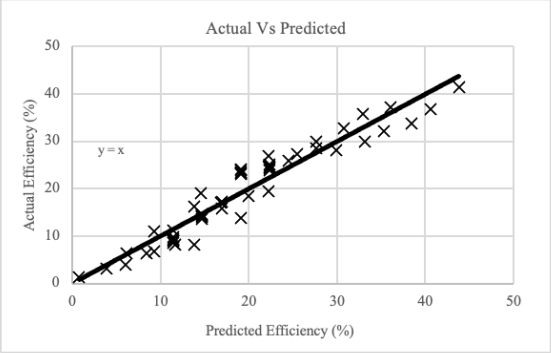


FIGURE 13. Parity plot for linear correlation of the actual and predicted removal efficiency

The link between various elements and the efficiency of oil removal was visually illustrated by a contour plot created with the help of the DE. The contour plot map produced when all the data was fed into statistical software is displayed in Figure 15.



FIGURE 14. Contour Plot for all experimental runs

The plot's darkest green regions represented ideal circumstances for removing the most oil. The optimal conditions for ultrasonic cleanup were determined by this exhaustive investigation. The importance of each criterion in terms of removal efficiency is compiled in Table 3.

TABLE 3. Summarized the significance of the experiment.

Significance	RE (%)	Condition
Most significant	41.39	Time: 15 minutes Power: 240W Ratio: 1:0.5 Salinity: Saline water
Least significant	1.30	Time: 5 minutes Power: 120W Ratio: 1:1.5 Salinity: Tap water

THERMO-GRAVIMETRIC ANALYSIS (TGA)

The TGA was started by understanding the Pyris™ software. Firstly, 10 mg of the untreated and treated sand were heated between 30 – 700 °C at a constant rate of 10 °C/min. Nitrogen gas will be purged at the rate of 20 mL/min at the same time. The percentage of weight loss using the TGA was calculated using the Eq. 5 shown below.

$$= \frac{(m_i - m_r)}{m_i} \times 100\% \quad (5)$$

The oil RE of the treated sand was calculated using the Eq. 6.

$$= \frac{(w_i - w_r)}{w_i} \times 100\% \quad (6)$$

The TGA was employed as a means of verifying the results obtained from the UV-Vis analysis. Samples from specific runs were analysed to determine the percentage of oil remaining after remediation. TGA data indicated a gradual decrease in oil content with increased remediation time, demonstrating the efficacy of the ultrasonic treatment. For example, the oil removal percentages for Run 31 (5 minutes), Run 32 (10 minutes), and Run 33 (15 minutes) were calculated as 11.0%, 53.0%, and 61.5%, respectively. These findings confirmed the hypothesis that extended ultrasonic exposure improves oil removal from polluted sand. By comparing the UV-Vis graphs for these three runs in Figure 15 and Figure 16, the graph's trend can be seen, which shows that as time passes, removal efficiency increases.

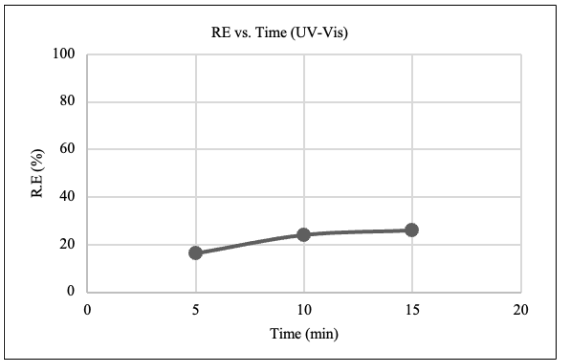


Figure 15. RE vs Time for UV-Vis Analysis

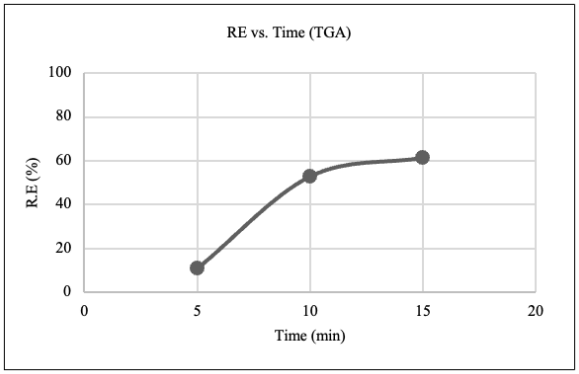


FIGURE 16. RE vs Time for TGA Analysis

CONCLUSION

This study demonstrates that ultrasonic treatment has meaningful potential to remediate the sand contaminated with used cooking oil (UCO). The effectiveness of the process was influenced by the combined effects of treatment time, ultrasonic power, oil–sand ratio, and the type of aqueous medium. Among the conditions investigated, the highest removal efficiency of 41.4% was achieved at an ultrasonic power of 240 W, a treatment time of 15 min, an oil–sand ratio of 1:0.5, and saline water as the treatment medium. In contrast, the lowest removal efficiency of 1.3% was obtained at 120 W, 5 min, an oil–sand ratio of 1:1.5 and tap water. Overall, longer treatment time, higher ultrasonic power, and the presence of salinity favoured oil removal, while the oil–sand ratio emerged as an important factor governing the overall remediation performance. The experimental observations were further supported by TGA analysis, which showed a progressive reduction in residual oil with increasing ultrasonic treatment time.

Beyond demonstrating the feasibility of ultrasonic remediation, this work provides a quantitative basis for predicting process performance. The developed linear regression model was able to estimate removal efficiency within the experimental range with a root mean square error of 2.73, indicating its usefulness as a preliminary predictive tool for selecting suitable operating conditions. Nevertheless, the present findings represent laboratory-scale conditions, and further investigation is required before the process can be translated to larger remediation systems. Future studies should therefore focus on improving removal efficiency, examining wider operating ranges, evaluating energy consumption and treatment cost, and validating the model at pilot scale. The integration of ultrasonic treatment with complementary techniques such as biodegradation or other environmentally compatible remediation processes may also provide opportunities for achieving greater oil removal. Overall, the findings contribute to the development of a practical and controllable approach for addressing UCO-contaminated sand while providing a foundation for future optimization and scale-up that was found to be $RE(\%)=14.62+1.29\alpha+0.0305\beta+7.19\gamma-22.68\delta$.

ACKNOWLEDGEMENT

The authors would like to express their sincere gratitude to Universiti Kuala Lumpur (UniKL) and Majlis Amanah Rakyat (MARA) for their financial support of this research. The funding provided has been instrumental in enabling the successful completion of this study. The authors also acknowledge UniKL for the institutional support, facilities, and research environment that contributed significantly to the execution of this work.

DECLARATION OF COMPETING INTEREST

None.

REFERENCES

Abousnina, R. & Lim Allister, R. 2022. Oil contaminated sand: Sources, properties, remediation, and engineering applications. In *Sand in Construction*. IntechOpen. https://doi.org/10.5772/intechopen.103802

Agarwal, A., Zhou, Y. & Liu, Y. 2016. Remediation of oil-contaminated sand with self-collapsing air microbubbles. *Environmental Science and Pollution Research* 23(23): 23876–23883. https://doi.org/10.1007/s11356-016-7601-5

Aliff Radzuan, M.R. 2017. *Removal of Oil Droplets from Oil-in-Water Mixtures by Dissolved Air Flotation (DAF)*. PhD thesis. University of Surrey, UK.

Aliff Radzuan, M.R., Abia-Biteo Belope, M.A. & Thorpe, R.B. 2016. Removal of fine oil droplets from oil-in-water mixtures by dissolved air flotation. *Chemical Engineering Research and Design* 115: 19–33. https://doi.org/10.1016/j.cherd.2016.09.013

Aliff Radzuan, M.R., Syed Hassan, S.N.S., Jamil, J., Mohamad Nasir, N.S. & Alikasturi, A.S. 2022. Removal of oil from oil-contaminated sand using chemical-free bubbles in turbulent and laminar flows: A conceptual paper. In *Proceedings of the 3rd International Conference on Green Environmental Engineering and Technology*, edited by Norazian Mohamed Noor, Sung Ting Sam & Aeslina Abdul Kadir, 313–318. Singapore: Springer.

Avvaru, B., Venkateswaran, N., Uppara, P., Iyengar, S.B. & Katti, S.S. 2018. Current knowledge and potential applications of cavitation technologies for the petroleum industry. *Ultrasonics Sonochemistry* 42: 493–507.

Abdul Wahab, A.A., Chang, S.H. & Md Som, A. 2015. Characterization of waste cooking oil as a potential green solvent for liquid-liquid extraction. In *International Conference on Advances in Civil and Environmental Engineering 2015*.

Befkadu, A.A. & Chen, Q. 2018. Surfactant-enhanced soil washing for removal of petroleum hydrocarbons from contaminated soils: A review. *Pedosphere* 28(3): 383–410. https://doi.org/10.1016/S1002-0160(18)60027-X

Checa-Fernández, A., Santos, A., Conte, L.O., Romero, A. & Domínguez, C.M. 2022. Enhanced remediation of a real HCH-polluted soil by the synergetic alkaline and ultrasonic activation of persulfate. *Chemical Engineering Journal* 440: 135901. https://doi.org/10.1016/j.cej.2022.135901

Choi, J., Lee, D. & Son, Y. 2021. Ultrasound-assisted soil washing processes for the remediation of heavy metals contaminated soils: The mechanism of the ultrasonic desorption. *Ultrasonics Sonochemistry* 74: 105574. https://doi.org/10.1016/j.ultsonch.2021.105574

Dabirian, R., Padsalgikar, A., Mohan, R.S. & Shoham, O. 2018. Four-layer model for prediction of sand bed height in horizontal gas-liquid stratified flow. *Journal of Petroleum Science and Engineering* 165: 151–160. https://doi.org/10.1016/j.petrol.2018.02.022

Daud, M.S.M., Ngadiman, N.I. & Suliman, M.S. 2020. The awareness of recycling the used of cooking oil. *Journal of Critical Reviews* 7(8): 30–32. https://doi.org/10.31838/jcr.07.08.06

Dehghani, M.H., Karri, R.R., Koduru, J.R., Manickam, S., Tyagi, I., Mubarak, N.M. & Suhas. 2023. Recent trends in the applications of sonochemical reactors as an advanced oxidation process for the remediation of microbial hazards associated with water and wastewater: A critical review. *Ultrasonics Sonochemistry* 94: 106302. https://doi.org/10.1016/j.ultsonch.2023.106302

den Engelsen, C.W., Isarin, J.C., Warmoeskerken, M.M.C.G. & Groot Wassink, J. 2002. Bubble size distribution of foam. *AUTEX Research Journal* 2(1): 14–27. https://doi.org/10.1515/aut-2002-020103

Drozdov, A.N., Drozdov, N.A., Bunkin, N.F. & Kozlov, V.A. 2017. Study of suppression of gas bubbles coalescence in the liquid for use in technologies of oil production and associated gas utilization. In *SPE Russian Petroleum Technology Conference 2017*. Society of Petroleum Engineers. https://doi.org/10.2118/187741-MS

Effendi, A.J., Wulandari, M. & Setiadi, T. 2019. Ultrasonic application in contaminated soil remediation. *Current Opinion in Environmental Science & Health* 12: 66–71. https://doi.org/10.1016/j.coesh.2019.09.009

Fagan, W.P. & Weavers, L.K. 2019. Sonochemical remediation of pollutants in soils and sediments. In *Encyclopedia of Water*, 1–21. Wiley. https://doi.org/10.1002/9781119300762.wsts0070

Feng, D. & Aldrich, C. 2000. Sonochemical treatment of simulated soil contaminated with diesel. *Advances in Environmental Research* 4(2): 103–112. https://doi.org/10.1016/S1093-0191(00)00008-3

Fraiese, A., Cesaro, A., Belgiorno, V., Sanromán, M.A., Pazos, M. & Naddeo, V. 2020. Ultrasonic processes for the advanced remediation of contaminated sediments. *Ultrasonics Sonochemistry* 67: 105171. https://doi.org/10.1016/j.ultsonch.2020.105171

Fuchs, F.J. 1995. Ultrasonic cleaning: Fundamental theory and application. In *Aerospace Environmental Technology Conference*. NASA Marshall Space Flight Center.

Jamil, J., Nordin, M.N., Yu, M. & Aliff Radzuan, M.R. 2021. Oily sand remediation concurrently with oil-in-water cleaning mechanisms using chemical-free microbubbles: A concept paper. *Materials Today: Proceedings* 31: A137–A140. https://doi.org/10.1016/j.matpr.2021.01.160

Jatnika Effendi, A. & Wulandari, M. 2019. The impact of ultrasonic power and time for the removal of total petroleum hydrocarbon from low permeability contaminated soils. *IOP Conference Series: Earth and Environmental Science* 314.

Kamaruzaman, N.H.I., Abdul Halim, N.S., Abdul Malek, N.H. & Idris, N.S.U. 2022. Households awareness and practices on used cooking oil recycling in Felda Lepar Hilir 1, Pahang. *IOP Conference Series: Earth and Environmental Science* 1102(1): 012073. https://doi.org/10.1088/1755-1315/1102/1/012073

King, W.G., Djun, L.M., Affam, A.C., Chung, W.C., Swee, W.C. & Adebayo, J.O. 2019. Application of hybrid ultrasonic cavitation/adsorption and coagulation for treatment of palm oil mill effluent. *AIP Conference Proceedings* 2124. https://doi.org/10.1063/1.5117068

Kováts, P., Thévenin, D. & Zähringer, K. 2020. Influence of viscosity and surface tension on bubble dynamics and mass transfer in a model bubble column. *International Journal of Multiphase Flow* 123: 103174. https://doi.org/10.1016/j.ijmultiphaseflow.2019.103174

Li, J., Song, X., Hu, G. & Thring, R.W. 2013. Ultrasonic desorption of petroleum hydrocarbons from crude oil contaminated soils. *Journal of Environmental Science and Health, Part A* 48(11): 1378–1389. https://doi.org/10.1080/10934529.2013.781885

Li, Y.T., Li, D., Lai, L.J. & Li, Y.H. 2020. Remediation of petroleum hydrocarbon contaminated soil by using activated persulfate with ultrasound and ultrasound/Fe. *Chemosphere* 238: 124657. https://doi.org/10.1016/j.chemosphere.2019.124657

Mat-Shayuti, M.S., Tuan Ya, T.M.Y.S., Abdullah, M.Z., Othman, N.H. & Alias, N.H. 2021. Exploring the effect of ultrasonic power, frequency, and load toward remediation of oil-contaminated beach and oilfield sands using ANOVA. *Environmental Science and Pollution Research* 28(41): 58081–58091. https://doi.org/10.1007/s11356-021-14776-8

Mohamed Noor, M.H., Mohd Azli, M.F.Z., Ngadi, N., Inuwa, I.M., Opotu, L.A. & Mohamed, M. 2022. Optimization of sonication-assisted synthesis of magnetic *Moringa oleifera* as an efficient coagulant for palm oil wastewater treatment. *Environmental Technology & Innovation* 25: 102191. https://doi.org/10.1016/j.eti.2021.102191

Ossai, I.C., Ahmed, A., Hassan, A. & Hamid, F.S. 2020. Remediation of soil and water contaminated with petroleum hydrocarbon: A review. *Environmental Technology & Innovation* 17: 100526. https://doi.org/10.1016/j.eti.2019.100526

Park, B. & Son, Y. 2017. Ultrasonic and mechanical soil washing processes for the removal of heavy metals from soils. *Ultrasonics Sonochemistry* 35: 640–645. https://doi.org/10.1016/j.ultsonch.2016.02.002

Peng, Y., Liu, Y., Dai, J., Cao, L. & Liu, X. 2020. A sustainable strategy for remediation of oily sewage: Clean and safe. *Separation and Purification Technology* 240: 116592. https://doi.org/10.1016/j.seppur.2020.116592

Rashid, F.L., Hussein, E.Q., Hussein, A.K. & Younis, O. 2023. Parametric study of single air bubble rising through different salinity water column using volume of fluid (VOF) technique. *Journal of Engineering Science and Technology* 18(1): 671–684.

Sivagami, K., Anand, D., Divyapriya, G. & Nambi, I. 2019. Treatment of petroleum oil spill sludge using the combined ultrasound and Fenton oxidation

process. *Ultrasonics Sonochemistry* 51: 340–349. https://doi.org/10.1016/j.ultsonch.2018.09.007

Sivakumar, S., Ravisankar, R., Raghu, Y., Chandrasekaran, A. & Chandramohan, J. 2012. FTIR spectroscopic studies on coastal sediment samples from Cuddalore District, Tamilnadu, India. *Indian Journal of Advances in Chemical Science* 1: 40–46.

United States Environmental Protection Agency. 2011. *Biodiesel*. United States Environmental Protection Agency.

Wan Azahar, W.N.A., Bujang, M., Putra Jaya, R., Hainin, M.R., Mohamed, A., Ngadi, N. & Jayanti, D.S. 2016. The potential of waste cooking oil as bio-asphalt for alternative binder—An overview. *Jurnal Teknologi* 78(4): 111–116. https://doi.org/10.11113/jt.v78.8007

Wulandari, M. & Effendi, A.J. 2018. Effect of frequency and ratio solid liquid on ultrasonic remediation of petroleum contaminated soil. *AIP Conference Proceedings* 2014(1): 020120. https://doi.org/10.1063/1.5054524

Xu, Y., Langbauer, C. & Hofstaetter, H. 2017. The application of ultrasonic technology for cleaning oil contaminated sand. In *SPE Asia Pacific Health, Safety, Security, Environment and Social Responsibility Conference*. Society of Petroleum Engineers. https://doi.org/10.2118/185261-MS

Yusof, N.S.M., Babgi, B., Alghamdi, Y., Aksu, M., Madhavan, J. & Ashokkumar, M. 2016. Physical and chemical effects of acoustic cavitation in selected ultrasonic cleaning applications. *Ultrasonics Sonochemistry* 29: 568–576. https://doi.org/10.1016/j.ultsonch.2015.06.013

Zhao, F., Yan, Q. & Cheng, D. 2021. Numerical study on the desorption processes of oil droplets inside oil-contaminated sand under cavitation micro-jets. *Ultrasonics Sonochemistry* 78: 105745. https://doi.org/10.1016/j.ultsonch.2021.105745

Zhou, G.-J., Lai, R.W.S., Sham, R.C.T., Lam, C.S., Yeung, K.W.Y., Astudillo, J.C., Ho, K.K.Y., Yung, M.M.N., Yau, J.K.C. & Leung, K.M.Y. 2019. Accidental spill of palm stearin poses relatively short-term ecological risks to a tropical coastal marine ecosystem. *Environmental Science & Technology* 53(21): 12269–12277. https://doi.org/10.1021/acs.est.9b04636